DNA stable isotope probing reveals contrasted activity and phenanthrene-degrading bacteria identity in a gradient of anthropized soils

Florian Lemmel, Florence F. Maunoury-Danger, Corinne Leyval, Aurélie Cebron

DNA stable isotope probing reveals contrasted activity and phenanthrene-degrading bacteria identity in a gradient of anthropized soils

Florian Lemmel[1], Florence Maunoury-Danger[2], Corinne Leyval[1] and Aurélie Cébron[1,†]

[1] *Université de Lorraine, CNRS, LIEC, F-54000, Nancy, FRANCE*

[2] *Université de Lorraine, CNRS, LIEC, F-57000 Metz, FRANCE*

[†] Corresponding author: aurelie.cebron@univ-lorraine.fr

Full postal address of the corresponding author: Dr. Aurélie Cébron, LIEC UMR7360, Faculté des Sciences et Technologies, Bd des Aiguillettes, BP70239, 54506 Vandoeuvre-les-Nancy Cedex, FRANCE.

Keywords: SIP; multi-contaminated soils; Illumina sequencing; ecology

ABSTRACT

Polycyclic aromatic hydrocarbons (PAHs) are ubiquitous soil organic pollutants. Although PAH-degrading bacteria are present in almost all soils, their selection and enrichment have been shown in historically high PAH contaminated soils. We can wonder if the effectiveness of PAH biodegradation and the PAH-degrading bacterial diversity differ among soils. The stable isotope probing (SIP) technique with ^{13}C-phenanthrene (PHE) as a model PAH was used to: i) compare for the first time a range of ten soils with various PAH contamination levels, ii) determine their PHE-degradation efficiency, and iii) identify the active PHE-degraders using 16S rRNA gene amplicon sequencing from ^{13}C-labelled DNA. Surprisingly, the PHE degradation rate was not directly correlated to the initial level of total PAHs and phenanthrene in the soils, but was mostly explained by the initial abundance and richness of soil bacterial communities. A large diversity of PAH-degrading bacteria was identified for seven of the soils, with differences among soils. In the soils where the PHE degradation activities were the higher, *Mycobacterium* species were always the dominant active PHE degraders. A positive correlation between PHE-degradation level and the diversity of active PHE-degraders (Shannon index) supported the hypothesis that cooperation between strains led to a more efficient PAH degradation.

INTRODUCTION

Polycyclic aromatic hydrocarbons (PAHs) are organic contaminants that represent a major source of environmental pollution, especially in soils. Anthropogenic activities are the main source of these contaminants due to the incomplete combustion of organic materials such as coke and petroleum

products during industrial processing. In industrial brownfields, although pollution stopped several decades ago, soil contamination can still reach very high levels (Biache *et al.* 2017). PAHs can accumulate in soils and be a serious threat for human health and ecosystem functioning with regard to their carcinogenicity and toxicity (Eom *et al.* 2007; Abdel-Shafy and Mansour 2016). However, the stress from high PAH concentrations leads to adaptation and selection of soil microbial communities (Bourceret *et al.* 2016). In these soils, a selection of microorganisms able to tolerate PAHs or degrade them has been shown (Cébron *et al.* 2008; Sawulski, Clipson and Doyle 2014), and involves detoxification (Sutherland 1992) or metabolism (PAHs used as a carbon source; Ghosal *et al.* 2016) mechanisms. Therefore, high levels of PAH contamination could impair soil functioning and lead to loss of functions (i.e. functions involved in C and N cycling; Liang *et al.* 2009). But it also leads to gain of functions (i.e. functions involved in PAH biodegradation; Cébron *et al.* 2008). Nevertheless, communities from weakly PAH-contaminated soils (soil background level) can also harbour the PAH degradation function (Crampon *et al.* 2017). Therefore, we can wonder if the effectiveness (i.e. the rate) of PAH biodegradation is similar between non- or low-contaminated soils on the one hand and soils with high and historical PAH contamination on the other hand. This aspect needs to be further explored to better understand the factors controlling the soil PAH biodegradation efficiency, which sometimes limits soil bioremediation (Chauhan *et al.* 2008; Ghosal *et al.* 2016).

In order to study the PAH biodegradation function, most studies have only sought to detect the presence of certain functional genes. PAH-RHDα genes, encoding the alpha subunit of PAH-ring hydroxylating dioxygenase enzymes involved in the first step of the bacterial biodegradation pathway, are choice targets indicating the functional potential of the microbial community (Cébron *et al.* 2008; Sawulski, Clipson and Doyle 2014), but this approach does not identify the actors of biodegradation. Stable isotope probing (SIP) is a culture-independent technique that links microbial identity with functions in complex systems such as soils (Dumont and Murrell 2005). This technique uses ^{13}C-labelled compounds and allows for the monitoring of ^{13}C during biodegradation and the labelling of cell components (e.g. DNA) of microbes using the ^{13}C labelled substrate as a carbon source for their growth. SIP has until now been extensively used to study the degradation of single carbon compounds (Dumont et al. 2006; Mosbaek et al. 2016; He et al. 2019), but more and more studies use SIP to decipher the pathways and actors involved in degradation of natural and anthropic complex compounds, such as cellulose/lignin (Wilhelm *et al*. 2019) and various organic pollutants (Li et al. 2015; Khawand et al. 2016), among which the PAHs, i.e. naphthalene, phenanthrene, pyrene (Cébron *et al.* 2011; Wald *et al.* 2015; Song *et al.* 2016; Guo *et al.* 2017; Thomas *et al.* 2019) in order to identify microbial degraders. However, only few investigations have been carried out on PAH degraders in weakly contaminated soils (Song *et al.* 2016; Chen *et al.* 2018), and we do not know whether their PAH-degrading bacterial diversity is similar to historically and highly PAH-contaminated

soils. Most studies have used SIP to compare the PAH degradation yield and degrader identity in one soil under various conditions. For example, certain authors sought to understand the impact of surfactants (Crampon *et al.* 2017; Guo *et al.* 2017), root exudates (Cébron *et al.* 2011; Lv *et al.* 2018; Thomas, Corre and Cébron 2019), or temperature (Wald *et al.* 2015). On the other hand, SIP was never used to study a wide range of soils and compare their communities of PAH degraders in order to see i) whether some taxa are more efficient at PAH degradation than others, and ii) whether historically contaminated soils harbour a different diversity of active microorganisms than weakly contaminated soils.

In this context, the aim of this study was to compare a range of ten soils displaying a gradient of anthropization, determine their PAH-degradation efficiency, and identify the active PAH degraders. Our hypothesis was to test whether i) the intensity of PAH degradation was correlated to the level of PAH contamination of the soils, ii) the microbial communities from historically and highly PAH-contaminated soils were more efficient than those from weakly polluted soils, and iii) PAH degrader identity could explain the differences in PAH degradation rates, involving more or less efficient taxa. Phenanthrene (PHE), which is widely distributed in the environment and in contaminated soils, was used as a model PAH in SIP experiments. PHE-degrading bacteria were identified using high-throughput 16S rRNA gene amplicon sequencing from ^{13}C-labelled DNA.

MATERIALS AND METHODS

Soil sampling and characteristics

The soils used in this study were collected in November 2015 from various woodland ecosystems located on industrial wastelands, natural forest or ancient gravel pits, located in the "Grand Est" region (north-east of France); all sites are located within a 50-km radius (**Figure S1**). At each of the 10 sites, samples were collected from three independent sub-sites 1 m apart. The three sub-site soil blocks were mixed to get one composite sample per site. Back to the laboratory, the soil samples were air-dried at room temperature for 1 week, and then sieved at 2 mm. All the dried and sieved soils were stored similarly at room temperature in the dark (6 months) before stable isotope probing experiment setup. Three soils were considered as weakly anthropized soils: two natural forest soils collected at Hémilly (He; Moselle) and Montiers-sur-Saulx (Mo; Meuse), and one anthropized but unpolluted ancient gravel pit soil collected at Dieulouard (Di; Meurthe-et-Moselle). Seven anthropized soils known to be polluted by metals and/or PAHs were collected from i) former slag heaps at Homécourt (Ho; Meurthe et-Moselle), Terville (Ter; Moselle), Uckange (Uc; Moselle), and Neuves-Maisons (NM; Meurthe-et-Moselle), and ii) former settling ponds at Pompey (Po; Meurthe-et-Moselle), Mont-St-Martin (MsM; Meurthe-et- Moselle) and Russange-Micheville (RM; Moselle).

This soil collection was chosen to cover a wide range of anthropization situations described in Lemmel *et al.* (2019). Briefly, a gradient of polycyclic aromatic hydrocarbon contamination was shown based on the 16 US-EPA PAHs ranging from 0.03 to 1,095.90 mg kg^{-1} dw soil (**Table 1**). The soils presented variable 16S rRNA gene abundances ranging from 4.4 to 41.5 x 10^{10} copies g^{-1}. The lowest and highest 16S rRNA gene abundances were found in the Uc and NM soils and the Po and Te soils, respectively, while the other soils presented intermediate abundance values. The soil bacterial communities were characterised by Illumina MiSeq sequencing, and indices describing alpha-diversity such as the Choa1 richness index were calculated (**Table S1**; Lemmel *et al.* 2019). The soils presented variable Chao1 richness indices ranging from 2,541 to 4,966, and the lowest and highest values were found in the RM and NM soils and Di and Ho soils, respectively. A gradient of metal contamination, mainly by Zn (60 to 119,000 mg kg^{-1}), Pb (23 to 39,500 mg kg^{-1}), and Cd (0.09 to 152 mg kg^{-1}), was also shown (**Table S1**). The pH, known to be one of the main drivers of microbial communities, was similar (from 7.2 to 8.0) among soils except for soil He (pH = 5.4). Other soil characteristics (Laboratoire d'analyse des sols, INRA, Arras, France), namely total organic carbon (24 to 159 g kg^{-1}), total nitrogen (0.56 to 7.19 g kg^{-1}), the C/N ratio (14 to 54), and texture (silty to sandy) varied among soils (**Table S1**; Lemmel *et al.* 2019).

Soil respiration

Basal respiration (BR) and substrate-induced respiration after PHE addition (PHE-SIR) were assessed, using two sets (i.e. unspiked and PHE-spiked) of soil samples. The two sets were prepared in triplicates, using 2.0 g dw of unspiked soil and of PHE-spiked soil, respectively. The PHE-spiked soil was prepared by mixing 1.8 g of soil with 0.2 g of spiked soil with PHE (Fluka, purity > 97.0 %) dissolved in n-hexane and left under a fume hood until complete evaporation of the solvent. The final PHE concentration was 200 mg kg^{-1}. Our experimental design included 60 samples (10 unspiked soils and PHE-spiked soils, in triplicates).

The two-gram soil samples were placed in 125-ml Plasma glass flasks and rewetted using sterilised water to reach 80 % water retention capacity (WRC). Then they were hermetically sealed with rubber-butyl corks and incubated in the dark at 24 °C (optimal temperature and humidity conditions) for 17 days for soil samples Di, MsM, Mo, NM, Te, and Uc and incubations were continued until 23 days for soil samples Ho, He, RM, and Po for which limited difference of respiration between BR and PHE-SIR could be observed. Respiration levels were monitored by measuring CO_2 contents using an infrared spectrophotometer (Binos, absorption at 2,325.6 cm^{-1}) on 4-ml fractions of the flask atmosphere sampled after 1, 2, 4, 7, 10, 14, 17, and 23 days of incubation using a syringe. Produced CO_2 was expressed as the carbon mass produced by one gram of dw soil per hour (mg of C g^{-1} h^{-1}).

The flasks were left open under the fume hood for 15 min to renew the atmosphere after each sampling.

Stable isotope probing incubations

For stable isotope probing (SIP) experiments, two sets of soil samples were prepared in triplicates by spiking all samples with PHE as described above. The first set was spiked with non-labelled PHE (i.e. ^{12}C-PHE; Fluka, > 97.0 % purity) and the second set was spiked with uniformly ^{13}C-labelled PHE (Sigma Aldrich, 99 atom % ^{13}C). Both sets were prepared twice: one was harvested at the beginning of the experiment (T0) and the other was incubated and harvested after 12 days (Tf). The SIP incubation experimental design included 120 samples (10 soils in triplicates, spiked with ^{12}C- or ^{13}C-PHE, and analysed at 2 time points T0 and Tf).

Each soil sample was placed in 125-ml Plasma glass flasks and rewetted using sterilised water to reach 80 % WRC. Then, the T0 samples were directly harvested by freezing at -80 °C. A CO_2 trap (2 ml of 1M NaOH in a 5-ml vial) was added in the Tf flasks before being hermetically sealed and incubated for 12 days in the dark at 24 °C, to avoid ^{13}C-CO_2 fixation (autotrophic and heterotrophic) during incubation. The atmosphere of the flasks was renewed once after 6 days, as described above. Tf incubations were harvested by freezing at -80 °C.

^{13}C-Phenanthrene degradation and ^{13}C-dissipation measurements

The soil samples (T0 and Tf) from SIP incubation stored at -80 °C were freeze-dried and ground to 500 µm with a grinder (Mixed Mill MM 400, Retsch) before PAH extraction, PHE-measurements and δ^{13}C estimation.

Total ~~PHE~~ PAH were extracted from one aliquot of ca. 500 mg of each dw soil with dichloromethane (DCM) at a high temperature (130 °C) and a high pressure (100 bars) using accelerated solvent extraction (DIONEX® 200 ASE), as described in Cennerazzo *et al.* (2017). Solvent extracts were evaporated under a nitrogen flow and dissolved in acetonitrile for PHE analysis. PHE was analysed by UV detection (254 nm) using a reverse-phase chromatography UHPLC DIONEX® Ultimate 3000 system equipped with a DAD (Diode Array Detector) and a Zorbax Eclipse PAH column (2.1 x 100 mm, 1.8 µm, Agilent). As some soils were already contaminated with aged PHE, the ^{13}C-PHE concentrations (^{13}C-PHE$_t$) at T0 or after 12 days were calculated as follow: ^{13}C-PHE$_t$ = PHE$_t$ - PHE$_i$, where PHE$_t$ is the total PHE concentration measured and PHE$_i$ is the initial PHE concentration of the soils before ^{13}C-PHE spiking.

Delta^{13}C measurements were performed at the PTEF platform (INRA, Champenoux, France). Briefly, $\delta^{13}C$ was measured from one aliquot of ca. 5 mg dw of soil using an elemental analyser (vario ISOTOPE cube, Elementar, Hanau, Germany) interfaced in line with a gas isotope ratio mass spectrometer (IsoPrime 100, Isoprime Ltd, Cheadle, UK; 0.2 ‰ sensitivity). $\delta^{13}C$ values were then transformed into $R^{13}C/^{12}C$ using the following formula: $R^{13}C/^{12}C = R_{vPDB} \times (1 + \delta^{13}C/1000)$, with R_{vPDB} equal to 0.0112375, value of the reference standard (Vienna Pee Dee Belemnite). From these calculated ratios, we determined the ^{13}C-dissipation corresponding to the percentage of ^{13}C content (coming from the ^{13}C-PHE) after the 12 days of incubation relative to the T0 ^{13}C content just after the spiking (representing 100%), taking also into account the natural $^{13}C/^{12}C$ ratio of the unspiked soils.

Available PAH content of unspiked soils was measured using cyclodextrin-based extraction and analysed by HPLC and UV-detection as described in Lemmel *et al.* (2019).

DNA extraction, isopycnic ultracentrifugation, and gradient fractionation

Total genomic DNA was extracted from ca. 300 mg of freeze-dried and ground ~~dw~~ soil (60 Tf samples from both ^{12}C and ^{13}C incubations) using a Fast DNA Spin Kit for Soil (MP Biomedicals, France), following the manufacturer's instructions. Then DNA was resuspended in 100 µl of DNase and pyrogen-free water. Concentration and purity (A_{260}/A_{280} ratio) were measured using a spectrophotometer (UV1800, Shimadzu) equipped with a TrayCell™ adapter (Hellma®). Heavy (^{13}C-labelled) DNA was separated from light (^{12}C) DNA according to the protocol described by Neufeld *et al.* (2007). Briefly, approximately 3,000 ng of DNA (except NM and Uc, for which 650 ng of DNA were used because lower genomic DNA quantities were recovered from these soils) were added to Quick-Seal polyallomer tubes (13 x 51 mm, 5.1 ml, Beckman Coulter), along with a gradient buffer (0.1M Tris-HCl, 0.1 M KCl, 1 mM EDTA) mixed with a CsCl solution, to a final buoyant density (BD) of ≈ 1.725 g ml^{-1}. The tubes were centrifuged at 42,400 rpm (i.e. 176,985 x g; VTI 65.2 rotor, Beckman) at 20 °C for 40 h. Following ultracentrifugation, 13 fractions of ca. 400 µl were collected from each tube using a fraction recovery system (Beckman). Then the BD value of each fraction was measured, and CsCl was removed by glycogen-assisted polyethylene glycol precipitation. DNA fractions were finally resuspended in 30 µl of TE buffer (pH 8.0).

Real-time quantitative PCR

In order to determine the distribution of heavy and light DNA and compare samples from ^{12}C and ^{13}C incubations, the abundance of 16S rRNA genes in each fraction was quantified using real-time quantitative PCR. The qPCR assay was performed as described in Cébron *et al.* (2008) by using the primer sets 968F/1401R (Felske, Akkermans and Vos 1998). Briefly, the reaction mixture (20 µl) was

composed of 10 µl of iQ SYBR green SuperMix (Bio-Rad), 0.8 µl of each primer (10 µM), 0.4 µl of bovine serum albumin (3%), 0.2 µl of dimethyl sulphoxide, 0.08 µl of T4gp32 (MP Biomedicals, France), and 1 µl of DNA as a template (DNA fraction samples or 10-fold dilution series from 10^8 to 10^1 copies μl^{-1} of the standard plasmid). Quantifications were performed using a CFX96 Real-Time PCR detection system (Bio-Rad), under the following conditions: an initial denaturation step at 95 °C for 5 min, and then 39 cycles of denaturation at 95 °C for 30 s, annealing at 56 °C for 20 s, extension at 72 °C for 30 s, and measurement of SYBR Green signal intensities at 82 °C for 5 s. Similarly, the abundance of 18S rRNA genes was quantified using the primer sets Fung5F/FF390R (Lueders *et al.* 2004) as previously described in Thion *et al.* (2012a).

Additionally, PAH-RHDα genes were also quantified in the genomic DNA from unspiked soils (before incubation) and in each DNA fraction (from the SIP assay) using the primer pairs PAH-RHDα GP-F/R for Gram-positive bacteria (Actinobacteria) and PAH-RHDα GN-F/R for Gram-negative bacteria (Proteobacteria) (Cébron *et al.* 2008). The reaction mixtures and quantification conditions were as described above except annealing temperatures that were 57 °C and 54 °C for PAH-RHDα GN and GP, respectively as described in Cébron *et al.* (2008).

Based on qPCR quantifications, the relative abundances of PAH-RHDα GP and GN genes (related to 16S rRNA genes) were calculated in unspiked soils. Similarly, the abundances of PAH-RHDα GP and GN genes in the soils after incubation and in the sequenced DNA fractions were calculated based on their average relative abundance in the light ^{12}C-DNA fraction and in the heavy ^{13}C-DNA fraction, respectively. All these gene relative abundance values are reported in **Table 1**.

Identification of phenanthrene-degrading bacteria

Based on the results of the distribution of heavy and light DNA in the recovered fractions, we observed an enrichment of the 16S rRNA gene in the heavy fraction (numbers 4-5-6; i.e. BD from 1.725 to 1.717 g ml^{-1}) of the soils incubated with ^{13}C-PHE, indicating a significant use of ^{13}C for bacterial growth. In order to identify these phenanthrene-degrading bacteria, 5 µl of the three heavy fractions were pooled from samples of both ^{12}C and ^{13}C incubations. These pooled fractions were used as templates to perform 16S rRNA gene amplicon libraries for Illumina MiSeq sequencing. To do so, the V3/V4 region of bacterial 16S rRNA genes (ca. 550 bp) was amplified using primers S-D-Bact-0341-a-S-17 and S-D-Bact-0787-b-A-20 (Muyzer, de Waal and Uitterlinden 1993; Caporaso *et al.* 2011), and following a previously described dual-index strategy (Kozich *et al.* 2013).

PCR reactions were performed on 1 µl of the pooled DNA fractions in a final volume of 50 µl, containing 10 µl of 5X Phusion HF buffer, 1.5 µl of 50 mM $MgCl_2$, 0.25 µl of DMSO, 0.1 µl of T4gp32 (MPBiomedicals, France), 0.1 µl of Phusion high-fidelity polymerase (Thermo Scientific), and 1 µl of each primer at 10 µM. PCR reactions were heated at 94 °C for 5 min, followed by 33 cycles of 30 s at

94 °C, 30 s at the annealing temperature (18 cycles starting at 63 °C, with a subsequent decrease of 0.5 °C at each cycle, and 15 cycles at 54 °C), 30 s at 72 °C, and a final extension step of 7 min at 72 °C. Amplification products were checked by 1% agarose gel electrophoresis and purified using the UltraClean-htp 96 Well PCR Clean-Up kit (Qiagen) following the manufacturer's instructions. After quantification using a Quant-iT Picogreen ds-DNA assay Kit (Invitrogen), an amplicon library was prepared as an equimolar pool of amplicons (10 nM), purified on a QIAquick PCR purification kit column (Qiagen), and sent for sequencing to Genewiz platform (South Plainfield, NJ, USA) using an Illumina MiSeq V2 Kit for 2 x 250 bp paired-end sequencing. Illumina MiSeq paired-end reads have been deposited in the SRA database under BioProject accession number PRJNA507956.

Sequence data were analysed following the MiSeq SOP procedure available in March 2017 and described in Kozich *et al.* (2013), using Mothur v.1.36.0 (Schloss *et al.* 2009). Due to the altered sequence quality of soil Uc as compared to the other 9 soils, two separate analyses were performed, with the Uc read treated separately from all the others. Paired-end reads were trimmed to a minimum QScore of 20 and joined using the following criteria: 404 bp < length < 480 bp, and a maximum of 6 ambiguous bases or no ambiguous base for paired-end reads from soil Uc or the other 9 soils, respectively. Alignment of unique sequences was performed against the Silva database. Chimeras were detected using Uchime (Edgar *et al.* 2011) and removed. Taxonomy was assigned using the Silva 132 bacteria database (released in Dec. 2017) using a cutoff of 80. Sequences affiliated to archaea, eukaryota, unknown, mitochondria, and chloroplasts were removed for further analysis. Singletons (sequences appearing only once among all samples) were removed. Sequences were clustered in Operational Taxonomic Units (OTUs) at 97% similarity. Finally, datasets were rarefied to the lowest number of sequences per sample (1,096 or 20,764 reads/sample for sequences from Uc or the other 9 soils, respectively).

Using a method describe by Thomas *et al.* (2019), active PHE-degraders were determined as OTUs present in the pooled heavy fractions of the ^{13}C-PHE incubation at a significantly higher abundance than in the pooled heavy fractions of the ^{12}C-PHE control incubation. We first selected major OTUs (i) represented by at least 5 sequences in each ^{13}C-PHE triplicate and (ii) with a higher average abundance in ^{13}C-PHE samples than in ^{12}C-PHE controls. After log-transformation, Welch's test followed by Benjamini-Hochberg correction of the p-values allowed determining the active PHE-degrading OTUs among major OTUs, separately for each soil. Statistically selected OTUs with exactly the same taxonomic affiliation were grouped and their sequence numbers were summed. For each soil, active PHE-degraders were reported with (i) their relative abundance related to the whole pool of PHE-degraders, (ii) their enrichment in ^{13}C-PHE heavy fractions compared to ^{12}C-PHE controls, and (iii) the corresponding number of OTUs in the groups.

Statistical analyses

All statistical analyses were performed using RStudio v1.1.442. Significant differences in PHE degradation, ^{13}C dissipation, and 16S rRNA gene copy numbers among soils were assessed by using Kruskal-Wallis rank sum test and the multiple comparison test included in the agricolae R package (Mendiburu 2017). Significant differences between PHE degradation and ^{13}C dissipation in a given soil were assessed using Welch's test. Linear correlations between all data were explored using the *rcorr* function included in the Hmisc package in R (Harell, Dupont and others 2018). Linear multiple regressions and factor interactions were explored using the lm function. Diversity indices were calculated using the *specnumber* and *diversity* functions included in the vegan package in R (Oksanen *et al.* 2017).

RESULTS

PAH contamination and PAH-dioxygenase genes of initial soils

The initial PAH and phenanthrene contents are presented in **Table 1**, together with PAH-RHDα gene relative abundances in the ten initial unspiked soils. Soil collection showed a gradient of total PAH contents ranging from 0.03 (He) to 1,095.90 mg kg^{-1} (NM) with ca. 1 to 10% of available PAHs (Lemmel *et al.* 2019). The initial unspiked soil PHE content followed a similar trend and ranged from below detection limit (He) to 199.24 mg kg^{-1} (Ho). We can note that highest initial available PAH and PHE contents were measured in Ho (54.14 and 18.10 mg kg^{-1}, respectively) and NM (82.98 and 15.77 mg kg^{-1}, respectively) soils. Based on the PAH content, we considered three groups of soil displaying low (< 20 mg kg^{-1}), medium (20 - 200 mg kg^{-1}), or high (> 200 mg kg^{-1}) PAH contamination. Interestingly, the relative abundance of PAH-RHDα genes in initial unspiked soils showed linear Pearson correlation with total soil PAH contents ($p = 2.62 \times 10^{-4}$, $r = 0.91$, and $p = 3.38 \times 10^{-8}$, $r = 0.99$ for the PAH-RHDα -GN and -GP genes, respectively) and available ones ($p = 5.77 \times 10^{-5}$, $r = 0.96$, and $p = 3.70 \times 10^{-6}$, $r = 0.98$ for the PAH-RHDα -GN and -GP genes, respectively).

Initial soil respiration

Depending on the soil activity, basal respiration (BR) and respiration induced after phenanthrene addition (PHE-SIR) were monitored for 17 or 23 days (**Figure S2**). Soils Mo, Te, and Po had the highest basal respiration activity. A globally higher CO_2 production was observed in the PHE-SIR flasks than in the BR flasks, except for soil He and Po. Soils Te, Di and Mo had the highest PHE-SIR level as compared to their BR, with the difference in CO_2 production between BR and PHE-SIR representing at the end more than 200 µgC per g of soil possibly indicating the complete mineralisation of the PHE (**Figure S2**). The Uc, MSM, NM, RM and Ho soils have lower CO_2 production representing between

90% (Uc) to 18% (Ho) of the corresponding C added through PHE spiking. Globally, after 10-12 days of incubation, most of the soils showed already a high difference in CO_2 production between the two conditions, indicating that most of the spiked phenanthrene had been degraded. Based on these results, we decided to stop SIP incubation after 12 days.

^{13}C-Phenanthrene degradation in the soils

We measured PHE concentrations and δ^{13}C levels to estimate ^{13}C-PHE degradation and ^{13}C dissipation in the soils at the end of SIP incubation (**Figure 1**). The soils presented variable percentages of ^{13}C-PHE degradation, ranging from 17.9% (RM) to 91.2% (Di) of the initial quantity of spiked ^{13}C-PHE. Soils Di and Po presented the highest PHE degradation, while soils RM and NM presented the lowest (Kruskal Wallis tests, $p = 0.002$). There was no correlation (Pearson) between the level of ^{13}C-PHE degradation and the soil characteristics (**Table S2**) and no correlation between ^{13}C-PHE degradation and the initial PAH and PHE contents (p-value of 0.21 and 0.59, respectively). Besides, medium PAH-polluted soils (Po, MsM, Te) presented higher ^{13}C-PHE degradation than low contaminated soils (He, Uc, Mo, RM, except Di) (Kruskal Wallis test, $p = 0.002$). Based on the soil δ^{13}C levels, we calculated ^{13}C dissipation in the soils; it ranged from 18.8% (NM) to 59.5% (Di) of the initial ^{13}C quantity, with significant differences (Kruskal Wallis test, $p = 0.002$). No correlation was found between ^{13}C dissipation and the soil characteristics, including the initial PAH and PHE contents (p-value of 0.16 and 0.52, respectively). Interestingly, the percentage of degraded PHE showed a positive linear correlation with both initial soil bacterial abundance (16S gene copy number; $P = 0.0001$, $R = 0.65$) and initial soil bacterial richness (Chao1 index; $P = 0.0002$, $R = 0.62$) (**Figure 2A and 2B**). A strong linear relationship ($p = 0.0004$; $R = 0.90$) was also found between the percentage of dissipated ^{13}C and degraded ^{13}C-PHE. The difference between the percentages of dissipated ^{13}C and degraded ^{13}C-PHE (**Figure 1**) indicate the amount of ^{13}C still present in the soil but not attributed to the remaining PHE (i.e. mainly ^{13}C-labeled microbial biomass) at the end of the incubations. Five soils (Di, Po, MsM, Te, and Ho) presented significantly higher PHE degradation than ^{13}C dissipation (Welch's test, $p < 0.05$), and this difference was positively correlated to the initial soil bacterial abundance (16S rRNA gene copy number) in the soils (Pearson; $p = 0.01$; $R = 0.76$).

Evidence of ^{13}C-labelled DNA

Bacterial 16S rRNA gene abundance was quantified from the DNA fractions obtained after ultracentrifugation of gDNA from the ^{12}C-PHE (control) and ^{13}C-PHE microcosms (**Figure 3**). The "heavy" DNA was in the fractions with a buoyant density ranging from 1.717 to 1.725 g ml^{-1}, while most of the "light" DNA corresponded to the fractions with a buoyant density ranging from 1.699 to 1.704 g ml^{-1}. The numbers of 16S rRNA gene copies were higher in the heavy DNA fractions collected

342 from the ^{13}C microcosms than in the ^{12}C controls, highlighting the presence of ^{13}C-labelled DNA
343 belonging to the active ^{13}C-PHE-degrading bacteria. This ^{13}C-DNA enrichment was observed for all
344 soils but Mo, and only a weak signal was observed for soil RM. 18S rRNA gene copies were also
345 quantified in all fractions (**Figure S3**), but no fungal ^{13}C-DNA enrichment was detected, indicating that
346 fungi were not significantly involved in PHE degradation or did not use carbon from PHE for their
347 growth, as they did not incorporate ^{13}C into their DNA.

348 In addition, PAH-RHDα-GN and -GP genes were also quantified in the DNA recovered from the CsCl
349 gradient fractions to calculate their relative abundance in the soils after incubation and in the
350 sequenced heavy ^{13}C-DNA fractions (**Table 1**). By comparing PAH-RHDα-GP and -GN abundances in
351 the soils before and after SIP incubation, we calculated a value of enrichment during incubation
352 (**Table 1**), ranging from 4 (NM) to 221 (Di) and from 3 (NM) to 126 (Te) for PAH-RHDα-GP and -GN,
353 respectively. Interestingly, PAH-RHDα-GP gene abundance and PAH-RHDα-GP gene enrichment in the
354 soils after SIP incubation were positively correlated to both the percentages of degraded PHE and
355 dissipated ^{13}C during SIP incubation (Pearson; $p = 0.03$, $R = 0.68$, and $p = 0.01$, $R = 0.75$, respectively,
356 for abundance; and $p = 0.005$, $R = 0.81$, and $p = 0.0006$, $R = 0.89$, respectively, for enrichment).
357 Additionally, PAH-RHDα-GP gene abundance in the heavy ^{13}C-DNA fractions was positively correlated
358 to the percentage of ^{13}C dissipated during SIP incubation (Pearson; $p = 0.02$, $R = 0.72$). No correlation
359 was found for PAH-RHDα-GN gene abundance in the soils after SIP incubation or in the ^{13}C-heavy
360 DNA fractions, or for PAH-RHDα-GN gene enrichment.

361

362 ## Identity of PHE degraders

363 Based on the results of the quantification of bacterial 16S rRNA genes, the pooled heavy DNA
364 fractions (**Figure 3**) were used as a template to prepare a 16S rRNA gene amplicon library for Illumina
365 sequencing. Due to the altered sequence quality of soil Uc as compared to the other 9 soils, two
366 separate analyses were performed, with Uc reads treated separately from all the other soils. Totals
367 of 7,150,234 and 405,380 reads were obtained after sequencing, and 3,485,709 and 22,402 reads
368 were kept after the trimming steps for the 9 soils and soil Uc (in triplicates and from ^{12}C and ^{13}C
369 incubations), respectively. Finally, data were rarefied to 20,764 and 1,096 reads/sample for the 9
370 soils and soil Uc, respectively.

371 Active PHE-degraders were determined as OTU present in the pooled heavy fractions of the ^{13}C-PHE
372 incubation at a significantly higher abundance than in the pooled heavy fractions of the
373 corresponding ^{12}C-PHE controls. Then, OTU corresponding to active PHE-degraders and sharing the
374 same taxonomic affiliation were gathered in groups. Relative abundance (relative to the whole pool

of PHE degraders) and enrichment (during ^{13}C-SIP incubation) are reported in **Figure 4** for each PHE-degrader group in the corresponding soil. Only 7 soils were reported in **Figure 4** as no OTU was detected with a significantly higher abundance in ^{13}C- than ^{12}C- heavy DNA fractions in He, Mo and RM soils, confirming the fact that we could not detect 16S rRNA gene copies number enrichment in heavy fractions of the ^{13}C-PHE incubations compared to the ^{12}C-PHE controls (**Figure 3**). A total of 2 (NM) to 12 (Di and Te) OTU groups (representing 3 to 30 OTUs) were highlighted as active PHE degraders. Most of these OTU groups were detected in ^{13}C-DNA fractions with enrichment higher than 10 times compared to the ^{12}C-controls. Active PHE degraders were relatively diverse and belonged to the Actinobacteria, Proteobacteria (α and β), Firmicutes, Patescibacteria and Cyanobacteria phyla; the last three were in minority compared to other phyla. Depending of the soil, dominant PHE degraders were mainly affiliated to *Micrococcaceae*, *Sphingomonadaceae* and *Burkholderiaceae* family, *Mycobacterium*, *Allorhizobium-Neorhizobium-Pararhizobium-Rhizobium (ANPR) and Massilia* genera, and *Arthobacter crystallopoietes, Rhizobium rhizogenes species.* Altogether, those 8 taxonomic groups represented 78% (Te) to 100% (MsM) on average of the whole active PHE degraders in the corresponding soil. Among Actinobacteria, OTUs affiliated to *Mycobacterium* were the major PHE degraders in soils Di (55%), Po (98%), and MsM (57%), while *Arthrobacter crystallopoietes* and Micrococcaceae family were the major PHE degraders in soil Te (44%) and NM (>99%), respectively. Besides, *Mycobacterium* affiliated OTUs were in the minority among the PHE degraders in both soils Te (20%) and Ho (4%). Concerning α-Proteobacteria, the *ANPR*, *Rhizobium rhizogenes* and Sphingomonadaceae family represented the second major PHE degrader groups in soil Di (34%), Uc (44%) and MsM (43%), respectively. Finally, among β-Proteobacteria, Burkholderiaceae family members were the major PHE degraders in soil Uc (51%), and more specifically the *Massilia* genus in soil Ho (87%).

The percentage of PHE degraded was positively correlated to the relative abundance of the globally most abundant PHE degrader, namely *Mycobacterium* ($p = 6.1 \times 10^{-5}$, $R = 0.76$; **Figure 2D**). For each soil replicate, we calculated diversity indices (i.e. species richness, Shannon diversity, and Pielou's evenness; **Table S3**) to describe the PHE-degrader community. Shannon diversity index of PHE-degraders was positively correlated to the percentage of degraded PHE ($p = 0.02$, $R = 0.48$; **Figure 2C**). The percentage of degraded PHE was not linearly correlated with the specific richness of PHE-degraders (**Figure 2E**). However, this relationship could be modeled by a saturation curve, suggesting a functional redundancy in the PHE-degrader community (beyond a certain species richness, several species have the same role in PHE degradation).

DISCUSSION

We evaluated the level of phenanthrene degradation and tried to identify the phenanthrene degraders in ten soils presenting a PAH pollution gradient. We hypothesised that the microbial communities of soils with a high and historical PAH contamination would be better adapted to PAH degradation than the ones from low- or non-contaminated soils. Consequently, the phenanthrene degradation rate would be positively correlated to the level of soil PAH contamination. Previous works indeed showed that greater PHE or PAH mineralisation appeared in soils pre-exposed to PAHs or with the highest PAH contamination level as compared to low- or non-contaminated soils (Johnsen and Karlson 2005; Carmichael and Pfaender 2009).

In the present study, we did not show any correlation between phenanthrene degradation rates and initial PAH or PHE contamination levels. Pre-exposure to PAH does not seem to be essential for efficient phenanthrene degradation. Nevertheless, this hypothesis was partly confirmed by the positive linear correlation between PAH-dioxygenase (both PAH-RHDα-GP and -GN) gene abundances and the total PAH contamination levels of the 10 soils. Our finding suggests that the selective pressure exerted by PAH pollution led to an enrichment in bacteria capable of PAH degradation. PAH-RHDα gene abundance is indeed a good indicator of the PAH contamination level in environmental samples (Cébron *et al.* 2008). However, although PHE degradation was surprisingly detected in all the tested soils, the PHE degradation rates were highly contrasted among soils and did not correlate with the PAH concentration or the PAH-dioxygenase gene abundance of the unspiked soils. Yet, although the moderately contaminated soil Di displayed higher PHE degradation than the non-contaminated ones, the highly contaminated soil NM did not display the highest PHE degradation rate. These results show that detecting the potential function (i.e. PAH-RHDα gene abundance) is not the sole predictor of the actual measured activity (i.e. PHE degradation) in the ten soils.

These differences in PHE biodegradation activity among soils could be explained by a myriad of abiotic and biotic factors specific to each soil, such as texture (Haghollahi et al. 2016), nutrient content (Breedveld and Sparrevik 2000), pH (Kästner et al. 1998), bioavailability of pollutants (Biache et al. 2017), multi-contamination (i.e. metal pollution; Sandrin and Maier 2003), and microbial diversity (Cébron et al. 2008).

Surprisingly, no correlation was found between the percentage of degraded PHE and any of the soil characteristics. No impact of the nitrogen or phosphorus contents or of the C:N ratio on the PHE degradation level was highlighted, even if it is well established that low nutrient levels limit microbial growth and activity (Wardle 1992) and hydrocarbon degradation (Leahy and Colwell 1990). C:N:P ratios could indeed drive PHE degradation (Smith, Graham and Cleland 1998) and the selection of active microorganisms in SIP experiments (Cébron *et al.* 2007); besides, adding N or P can increase the soil respiration (Breedveld and Sparrevik 2000) and improve the biodegradation of crude oil or gasoline (Leahy and Colwell 1990) and of PAHs (Joner *et al.* 2002; Jones *et al.* 2008) in soils.

Moreover, one of the main drivers of soil PAH degradation is PAH availability, mostly impacted by the soil texture (Carmichael and Pfaender 2009), organic matter type and content (Dictor *et al.* 2003), and the presence of aged pollution (Biache *et al.* 2008). Dictor *et al.* (2003) showed that even after a short period (i.e. few hours), a significant part of the spiked PHE became unavailable for soil microorganisms, resulting in reduced degradation. We can thus hypothesise that spiked PHE availability differed depending on the soils. The PHE degradation rate was well predicted from the mineralization data of soil spiked with PHE compared to the basal mineralization, except for the soil Mo where we overestimated it from mineralization pre-experiments. For Ho and NM soil, where the initial PAH contamination was the highest, the difference in mineralisation was low compared to the PHE degradation rates. This phenomenon could be due to the adaptation of bacterial communities in these aged PAH contaminated soils, leading to a shift in mineralization from the aged carbon (mostly PAHs) to the fresh added PHE by the same bacteria.

We also hypothesised that differences in PHE degradation rates between soils may be explained by the diversity of PHE degraders and/or by the presence of specific taxa with a higher PHE-degrading activity. In addition to the analysis of the diversity of the whole bacterial community in unspiked soils (Lemmel *et al.* 2019), the use of stable isotope probing allowed us to directly link the ^{13}C-PHE degradation function with the diversity of ^{13}C-labeled PHE degraders.

We get a very original result showing that the PHE degradation level was positively correlated to both bacterial abundance and bacterial richness of the initial soils, previously measured on unspiked soils (Lemmel *et al.* 2019). This relationship could be explained by i) the fact that soils harbouring a more abundant and diversified microbial community might contain more PHE-degrading bacteria (the sampling effect hypothesis, e.g. Hector *et al.* 2002) resulting in higher PHE degradation rates, or ii) facilitation between species improving PHE degradation. As broadly described in plant community ecology (Hooper and Vitousek 1998; Caldeira *et al.* 2001), facilitation between species enhances an ecosystem function and may be the mechanism responsible for the positive relationship between taxonomic diversity and ecosystem processes. We can consider that some bacterial species indirectly contributed to increase PHE degradation by facilitating the PHE degrader activity in the soil (for example by increasing their access to essential elements or by reducing the toxicity due to a high soil metal content). Our finding is in agreement with previous finding in microbial ecology. Jung et al. (2016) showed that a large proportion of functional gene categories were significantly altered by a reduction in microbial biodiversity, even if these authors also found that the efficiency of diesel biodegradation was increased in the low-diversity community suggesting that the relationship between microbial diversity and ecological function involves trade-offs among ecological processes.

PHE degradation activity was also positively correlated with the active PHE-degrader Shannon diversity index calculated from SIP data, but no correlation was found with PHE-degrader richness.

Complementarity between species for the use of PHE should be considered here. When the diversity of PHE-degrading species increases, the use of PHE as a carbon substrate is optimized and a greater amount of PHE is degraded. For example, PHE degradation results from a sum of reactions (Ghosal *et al.* 2016), and when the diversity of PHE degraders increases, the joint functioning of the different species ensures a greater number of its reactions and thus maximises PHE degradation. Thomas, Corre and Cébron (2019) recently demonstrated, using SIP combined to metagenomic analysis, that active PHE-degraders act in a consortium, whereby complete PHE mineralization is achieved through the combined activity of taxonomically diverse co-occurring bacteria performing successive metabolic steps. Similarly, positive relationships between species diversity and soil respiration (Bell *et al.* 2005) or the efficiency of hydrocarbon biodegradation in marine sediment (Dell'Anno *et al.* 2012) have been observed. All these observations refer to well-known ecological concept where increased microbial diversity corresponds to increased catabolic potential and, hence, to better removal of metabolites and pollutants as explained by Dejonghe *et al.* (2001). The positive correlation found with Shannon diversity index, and not with PHE-degrader species richness, tends to show that PHE degradation efficiency depends of the presence of keystone species, that if they are absent, greatly decreases the biodegradation rate. Indeed, below 10 active PHE-degrading OTUs, the PHE degradation rate is low, but when at least 10 OTUs are active in even proportion the PHE degradation is higher, leading to a more efficent PHE removal. This phenomenon was previously observed for other organic pollutants such as atrazine (Monard *et al.* 2011).

Through labelling of microbes metabolizing PHE and their degradation by-products, DNA-SIP allowed us identifying the active PHE-degraders in the studied soils. For three soils (He, Mo and RM), apparently, the ^{13}C-PHE degradation was too low and PHE-degraders growth too weak to generate a sufficient ^{13}C-labeling of the microbial biomass. Indeed, we could not detect significant enrichment of ^{13}C-DNA in heavy fractions of the CsCl gradients and, even after sequencing of the heavy DNA fractions, no OTUs could be detected as significantly enriched in the ^{13}C-PHE condition compared to the ^{12}C controls. When looking at the 7 other soils, a large number of bacterial OTUs was identified as PHE degraders (from 3 to 30 OTUs per soil representing 31 taxonomic groups). We found that the presence of some taxa seems to maximise the PHE degradation rate. Among them, the *Mycobacterium*, *Massilia*, *Arthrobacter, ANPR and Rhizobium* genera, and unclassified OTUs belonging to Sphingomonadaceae, Burkholderiaceae and Micrococcaceae seemed to be the main PHE degraders best explaining the PHE degradation rates in the 7 soils. PHE-degrading *Massilia* were isolated from soils after PHE exposure (Bodour *et al.* 2003; Zhang *et al.* 2010), and from PAH-polluted soils (Baquiran *et al.* 2012; Wang *et al.* 2016), or were detected in an oilfield by metagenomics (Zhou *et al.* 2017). Although no detailed information is available about the role and potential of *Massilia sp.* in PAH degradation in environmental samples, one study showed that *Massilia sp.* strain WF1 had

high degradation ability and tolerance to PHE (Gu *et al.* 2016). Additionally, *Massilia* seems to also tolerate metal contamination (Zhang *et al.* 2016). Micrococcaceae and among which *Arthrobacter* genus has been shown for its PAH degradation capacity both in pure culture (Aryal and Liakopoulou-Kyriakides 2013) and in the environment (Thion *et al.* 2012b). Similarly to our result, a recent study of Storey *et al.* (2018) showed also a strong increase of one unclassified OTU affiliated to Micrococcaceae family, being dominant in a soil after PHE amendment. *ANPR* genera, which relate to N-fixing bacteria through symbiosis with legumes, contain various *Rhizobium* species described for their capacity to tolerate and degrade PAHs (Poonthrigpun *et al.* 2006; González-Paredes *et al.* 2013), and have been used to enhance PAH phytoremediation (Johnson, Anderson and McGrath 2005; Teng *et al.* 2011). Members of the Sphingomonadaceae family are also well-known PAH degraders (Thomas, Corre and Cébron 2019) and many isolates belonging to Sphingomonadaceae were frequently isolated from PAH-contaminated environments (Johnsen, Wick and Harms 2005). Similarly, Burkholderiaceae family is known to contain various bacteria able to grow on PAHs or having PAH degradation genes, such as members of *Burkholderia* and *Ralstonia* genera (Fuenmayor *et al.* 1998; Cébron *et al.* 2008; Andreolli *et al.* 2011), and recently members of *Cupriavidus* genus (Kuppusamy *et al.* 2016; Oyehan and Al-Thukair 2017).

OTUs affiliated to the *Mycobacterium* (Actinobacteria) genus were the dominant PHE degraders in the soils displaying the higher PHE degradation rates. The PHE degradation rate was positively correlated to the relative abundance of OTUs affiliated to *Mycobacterium*. This relationship confirmed that *Mycobacterium* strains were essential drivers of PHE degradation in our soils and could be defined as a key stone species for efficient PHE-degradation. Due to their prevalence in many PAH-contaminated soils, *Mycobacterium* species have been suggested to potentially play a major role in the natural attenuation of PAHs (Cheung and Kinkle 2001; Chen, Peng and Duan 2016; Chen *et al.* 2018). Numerous *Mycobacterium* species have indeed been described for their ability to degrade various low- and high-molecular-weight PAHs, in PAH-contaminated soils (Chen *et al.* 2018; Li *et al.* 2018). Previous studies suggest that PAH-degrading *Mycobacterium* are well adapted to oligotrophic and low PAH availability conditions, usually found in PAH-contaminated soils. *Mycobacterium* can degrade PAHs under optimal conditions (C:N:P ratio of 100:10:1) as well as under N and P excess or deficiency (Leys *et al.* 2005). Additionally, Miyata *et al.* (2004) suggested that both passive diffusion and high-affinity transport systems contributed to the PHE uptake by *Mycobacterium* strain RJGII-135, and enabled the bacterium to use aqueous-phase PHE in high and low concentrations. Moreover, *Mycobacterium* strains can attach on the PAH source and form biofilms which increase PAH bioavailability (Bastiaens *et al.* 2000; Wick *et al.* 2002). Given that *Mycobacterium* were highlighted as main active PHE degraders in our soils presenting high PHE degradation rate, and that numerous studies describe *Mycobacterium* strains with PAH degradation

capacity, their presence could constitute a relevant indicator of PAH degradation. Further, they might be of interest for bioaugmentation of PAH degradation in contaminated environments.

CONCLUSION

For the first time we studied in parallel and through stable isotope probing the degradation of ^{13}C-phenanthrene in a collection of 10 anthropized soils presenting a PAH pollution gradient and identified major active phenanthrene degraders for 7 soils of the collection. Surprisingly, the phenanthrene degradation rate was neither correlated to the initial soil PAH contamination level nor to the functional PAH-degradation potential (occurrence of PAH-RHDα genes) but was best explained by the initial soil bacterial community richness and abundance. No specific taxa, representative of aged and highly contaminated soils, were identified. In the studied soils, the phenanthrene degradation efficiency depended on two parameters: i) to have a wide diversity of active phenanthrene degraders (correlation between PHE degradation and Shannon diversity index of active taxa) and ii) to have representatives of the *Mycobacterium* genus as dominant phenanthrene degrading taxa (correlation between PHE degradation and *Mycobacterium* occurrence). To conclude, our study shows that microbial community characteristics and the presence of specific key-stone species (*Mycobacterium*), but also species complementarity are more important for PAH degradation efficiency than initial levels of soil PAH contamination and the initial PAH-degradation potential.

ACKNOWLEDGEMENTS

This work was supported by the French national program EC2CO (Ecobios project), and the OSU-OteLo (TraitMic project). We thank Dr. S. Uroz (Labex Arbre, INRA Champenoux) for giving us access to the ultracentrifuge equipment. We would like to thank Arcelor Mittal, EPFL, GISFI, ONF, and LTO of Montiers (ANDRA/INRA, M.P. Turpault) for giving us access to the different sampling sites. We would like to thank C. Friry, G. Kitzinger and D. Billet (LIEC, Nancy, France) for technical assistance.

Authors have no conflicts of interest to declare.

REFERENCES

Abdel-Shafy HI, Mansour MSM. A review on polycyclic aromatic hydrocarbons: Source, environmental impact, effect on human health and remediation. *Egypt J Pet* 2016;**25**:107–23.

Andreolli M, Lampis S, Zenaro E *et al.* Burkholderia fungorum DBT1: a promising bacterial strain for bioremediation of PAHs-contaminated soils. *FEMS Microbiol Lett* 2011;**319**:11–8.

Aryal M, Liakopoulou-Kyriakides M. Biodegradation and Kinetics of Phenanthrene and Pyrene in the Presence of Nonionic Surfactants by Arthrobacter Strain Sphe3. *Water Air Soil Pollut* 2013;**224**:1426.

Baquiran JP, Thater B, Songco K *et al.* Characterization of Culturable PAH and BTEX Degrading Bacteria from Heavy Oil of the Rancho La Brea Tarpits. *Polycycl Aromat Compd* 2012;**32**:600–14.

Bastiaens L, Springael D, Wattiau P *et al.* Isolation of adherent polycyclic aromatic hydrocarbon (PAH)-degrading bacteria using PAH-sorbing carriers. *Appl Environ Microbiol* 2000;**66**:1834–43.

Bell T, Newman JA, Silverman BW *et al.* The contribution of species richness and composition to bacterial services. *Nature* 2005;**436**:1157–60.

Biache C, Mansuy-Huault L, Faure P *et al.* Effects of thermal desorption on the composition of two coking plant soils: Impact on solvent extractable organic compounds and metal bioavailability. *Environ Pollut* 2008;**156**:671–7.

Biache C, Ouali S, Cébron A *et al.* Bioremediation of PAH-contamined soils: Consequences on formation and degradation of polar-polycyclic aromatic compounds and microbial community abundance. *J Hazard Mater* 2017;**329**:1–10.

Bodour AA, Wang JM, Brusseau ML *et al.* Temporal change in culturable phenanthrene degraders in response to long-term exposure to phenanthrene in a soil column system. *Environ Microbiol* 2003;**5**:888–95.

Bourceret A, Cébron A, Tisserant E *et al.* The Bacterial and Fungal Diversity of an Aged PAH- and Heavy Metal-Contaminated Soil is Affected by Plant Cover and Edaphic Parameters. *Microb Ecol* 2016;**71**:711–24.

Breedveld GD, Sparrevik M. Nutrient-limited biodegradation of PAH in various soil strata at a creosote contaminated site. *Biodegradation* 2000;**11**:391–9.

Caldeira MC, Ryel RJ, Lawton JH *et al.* Mechanisms of positive biodiversity–production relationships: insights provided by δ13C analysis in experimental Mediterranean grassland plots. *Ecol Lett* 2001;**4**:439–43.

Caporaso JG, Lauber CL, Walters WA *et al.* Global patterns of 16S rRNA diversity at a depth of millions of sequences per sample. *Proc Natl Acad Sci U S A* 2011;**108 Suppl 1**:4516–22.

Carmichael LM, Pfaender FK. Polynuclear aromatic hydrocarbon metabolism in soils: Relationship to soil characteristics and preexposure. *Environ Toxicol Chem* 2009;**16**:666–75.

Cébron A, Bodrossy L, Stralis-Pavese N *et al.* Nutrient Amendments in Soil DNA Stable Isotope Probing Experiments Reduce the Observed Methanotroph Diversity. *Appl Env Microbiol* 2007;**73**:798–807.

Cébron A, Louvel B, Faure P *et al.* Root exudates modify bacterial diversity of phenanthrene degraders in PAH-polluted soil but not phenanthrene degradation rates. *Environ Microbiol* 2011;**13**:722–36.

Cébron A, Norini M-P, Beguiristain T *et al.* Real-Time PCR quantification of PAH-ring hydroxylating dioxygenase (PAH-RHDα) genes from Gram positive and Gram negative bacteria in soil and sediment samples. *J Microbiol Methods* 2008;**73**:148–59.

Cennerazzo J, de Junet A, Audinot J-N *et al.* Dynamics of PAHs and derived organic compounds in a soil-plant mesocosm spiked with 13C-phenanthrene. *Chemosphere* 2017;**168**:1619–27.

Chauhan A, Fazlurrahman, Oakeshott JG *et al.* Bacterial metabolism of polycyclic aromatic hydrocarbons: strategies for bioremediation. *Indian J Microbiol* 2008;**48**:95–113.

Chen S, Peng J, Duan G. Enrichment of functional microbes and genes during pyrene degradation in two different soils. *J Soils Sediments* 2016;**16**:417–26.

Chen S-C, Duan G-L, Ding K *et al.* DNA stable-isotope probing identifies uncultivated members of Pseudonocardia associated with biodegradation of pyrene in agricultural soil. *Fems Microbiol Ecol* 2018;**94**:fiy026.

Cheung P-Y, Kinkle BK. Mycobacterium Diversity and Pyrene Mineralization in Petroleum-Contaminated Soils. *Appl Environ Microbiol* 2001;**67**:2222–9.

Crampon M, Cebron A, Portet-Koltalo F *et al.* Low effect of phenanthrene bioaccessibility on its biodegradation in diffusely contaminated soil. *Environ Pollut* 2017;**225**:663–73.

Dejonghe W, Boon N, Seghers D *et al.* Bioaugmentation of soils by increasing microbial richness: missing links. *Environ Microbiol* 2001;**3**:649–57.

Dell'Anno A, Beolchini F, Rocchetti L *et al.* High bacterial biodiversity increases degradation performance of hydrocarbons during bioremediation of contaminated harbor marine sediments. *Environ Pollut* 2012;**167**:85–92.

Dictor MC, Berne N, Mathieu O *et al.* Influence of Ageing of Polluted Soils on Bioavailability of Phenanthrene. *Oil Gas Sci Technol* 2003;**58**:481–8.

Dumont MG, Murrell JC. Stable isotope probing - linking microbial identity to function. *Nat Rev Microbiol* 2005;**3**:499–504.

Dumont MG, Radajewski SM, Miguez CB *et al*. Identification of a complete methane monooxygenase operon from soil by combining stable isotope probing and metagenomic analysis. *Environ Microbiol* 2006;**8**:1240-1250.

Edgar RC, Haas BJ, Clemente JC *et al.* UCHIME improves sensitivity and speed of chimera detection. *Bioinforma Oxf Engl* 2011;**27**:2194–200.

Eom IC, Rast C, Veber AM *et al.* Ecotoxicity of a polycyclic aromatic hydrocarbon (PAH)-contaminated soil. *Ecotoxicol Environ Saf* 2007;**67**:190–205.

Felske A, Akkermans ADL, Vos WMD. Quantification of 16S rRNAs in Complex Bacterial Communities by Multiple Competitive Reverse Transcription-PCR in Temperature Gradient Gel Electrophoresis Fingerprints. *Appl Environ Microbiol* 1998;**64**:4581–7.

Fuenmayor SL, Wild M, Boyes AL *et al.* A gene cluster encoding steps in conversion of naphthalene to gentisate in Pseudomonas sp. strain U2. *J Bacteriol* 1998;**180**:2522–30.

Ghosal D, Ghosh S, Dutta TK *et al.* Current State of Knowledge in Microbial Degradation of Polycyclic Aromatic Hydrocarbons (PAHs): A Review. *Front Microbiol* 2016;**7**, DOI: 10.3389/fmicb.2016.01369.

González-Paredes Y, Alarcón A, Almaraz Juan J *et al.* Tolerance, growth and degradation of phenanthrene and benzo[a]pyrene by Rhizobium tropici CIAT 899 in liquid culture medium. *Appl Soil Ecol* 2013;**63**:105–11.

Gu H, Lou J, Wang H *et al.* Biodegradation, Biosorption of Phenanthrene and Its Trans-Membrane Transport by Massilia sp. WF1 and Phanerochaete chrysosporium. *Front Microbiol* 2016;**7**, DOI: 10.3389/fmicb.2016.00038.

Guo G, Tian F, Ding K *et al.* Bacterial Communities Predominant in the Degradation of C-13-Labeled Pyrene in Red Soil. *Soil Sediment Contam* 2017;**26**:709–21.

Haghollahi A, Fazaelipoor MH, Schaffie M. The effect of soil type on the bioremediation of petroleum contaminated soils. *J Environ Manag* 2016;**180**:197-201.

Harell FE, Dupont C, others with contributions from CD and many. *Hmisc: Harrell Miscellaneous*., 2018.

He D, Zhang L, Dumont MG *et al*. The response of methanotrophs to additions of either ammonium, nitrate or urea in alpine swamp meadow soil as revealed by stable isotope probing. *FEMS microbiol ecol 2019;**95***:fiz077.

Hector A, Bazeley-White E, Loreau M *et al.* Overyielding in grassland communities: testing the sampling effect hypothesis with replicated biodiversity experiments. *Ecol Lett* 2002;**5**:502–11.

Hooper DU, Vitousek PM. Effects of Plant Composition and Diversity on Nutrient Cycling. *Ecol Monogr* 1998;**68**:121–49.

Johnsen AR, Karlson U. PAH Degradation Capacity of Soil Microbial Communities: Does It Depend on PAH Exposure? *Microb Ecol* 2005;**50**:488–95.

Johnsen AR, Wick LY, Harms H. Principles of microbial PAH-degradation in soil. *Environ Pollut* 2005;**133**:71–84.

Johnson DL, Anderson DR, McGrath SP. Soil microbial response during the phytoremediation of a PAH contaminated soil. *Soil Biol Biochem* 2005;**37**:2334–6.

Joner EJ, Corgié SC, Amellal N *et al.* Nutritional constraints to degradation of polycyclic aromatic hydrocarbons in a simulated rhizosphere. *Soil Biol Biochem* 2002;**34**:859–64.

Jones MD, Singleton DR, Carstensen DP *et al.* Effect of incubation conditions on the enrichment of pyrene-degrading bacteria identified by stable-isotope probing in an aged, PAH-contaminated soil. *Microb Ecol* 2008;**56**:341–9.

690 Jung J, Philippot L, Park W. Metagenomic and functional analyses of the consequences of reduction
691 of bacterial diversity on soil functions and bioremediation in diesel-contaminated
692 microcosms. *Sci Rep* 2016;**6**:23012.

693 Kästner M, Breuer-Jammali M, Mahro B. Impact of inoculation protocols, salinity, and pH on the
694 degradation of polycyclic aromatic hydrocarbons (PAHs) and survival of PAH-degrading
695 bacteria introduced into soil. *App. Environ Microbiol* 1998;**64**:359-362.

696 Khawand ME, Crombie AT, Johnston A *et al*. Isolation of isoprene degrading bacteria from
697 soils,development of isoA gene probes and identificationof the active isoprene degrading soil
698 communityusing DNA-stable isotope probing. *Environ Microbiol* 2016;**18**:2743–2753.

699 Kozich JJ, Westcott SL, Baxter NT *et al.* Development of a Dual-Index Sequencing Strategy and
700 Curation Pipeline for Analyzing Amplicon Sequence Data on the MiSeq Illumina Sequencing
701 Platform. *Appl Environ Microbiol* 2013;**79**:5112–20.

702 Kuppusamy S, Thavamani P, Megharaj M *et al.* Polyaromatic hydrocarbon (PAH) degradation
703 potential of a new acid tolerant, diazotrophic P-solubilizing and heavy metal resistant
704 bacterium Cupriavidus sp. MTS-7 isolated from long-term mixed contaminated soil.
705 *Chemosphere* 2016;**162**:31–9.

706 Leahy JG, Colwell RR. Microbial degradation of hydrocarbons in the environment. *Microbiol Rev*
707 1990;**54**:305–15.

708 Lemmel F, Maunoury-Danger F, Fanesi A *et al.* Soil Properties and Multi-Pollution Affect Taxonomic
709 and Functional Bacterial Diversity in a Range of French Soils Displaying an Anthropisation
710 Gradient. *Microb Ecol* 2019;**77**:993–1013.

711 Leys NM, Bastiaens L, Verstraete W *et al.* Influence of the carbon/nitrogen/phosphorus ratio on
712 polycyclic aromatic hydrocarbon degradation by Mycobacterium and Sphingomonas in soil.
713 *Appl Microbiol Biotechnol* 2005;**66**:726–36.

714 Li J, Luo C, Zhang D *et al.* Autochthonous Bioaugmentation-Modified Bacterial Diversity of
715 Phenanthrene Degraders in PAH-Contaminated Wastewater as Revealed by DNA-Stable
716 Isotope Probing. *Environ Sci Technol* 2018;**52**:2934–44.

717 Li X, Lin Z, Luo C, Bai J *et al*. Enhanced microbial degradation of pentachlorophenol from soil in the
718 presence of earthworms: Evidence of functional bacteria using DNA-stable isotope probing.
719 *Soil Biol Biochem* 2015;**81**:168-177.

720 Liang Y, Li G, Nostrand JDV *et al.* Microarray-based analysis of microbial functional diversity along an
721 oil contamination gradient in oil field. *FEMS Microbiol Ecol* 2009;**70**:324–33.

722 Lueders T, Wagner B, Claus P *et al.* Stable isotope probing of rRNA and DNA reveals a dynamic
723 methylotroph community and trophic interactions with fungi and protozoa in oxic rice field
724 soil. *Environ Microbiol* 2004;**6**:60–72.

725 Lv X, Kankan Z, Li H *et al.* Niche partition of phenanthrene-degrading bacteria along a Phragmites
726 australis rhizosphere gradient. *Biol Fertil Soils* 2018;**54**:607–16.

727 Mendiburu F de. *Agricolae: Statistical Procedures for Agricultural Research*., 2017.

728 Miyata N, Iwahori K, Foght JM *et al.* Saturable, Energy-Dependent Uptake of Phenanthrene in
729 Aqueous Phase by Mycobacterium sp. Strain RJGII-135. *Appl Env Microbiol* 2004;**70**:363–9.

730 Monard C, Vandenkoornhuyse P, Le Bot B *et al.* Relationship between bacterial diversity and function
731 under biotic control: the soil pesticide degraders as a case study. *Isme J* 2011;**5**:1048–56.

732 Mosbæk F, Kjeldal H, Mulat DG *et al*. Identification of syntrophic acetate-oxidizing bacteria in
733 anaerobic digesters by combined protein-based stable isotope probing and metagenomics.
734 *ISME journal* 2016;**10**:2405.

735 Muyzer G, de Waal EC, Uitterlinden AG. Profiling of complex microbial populations by denaturing
736 gradient gel electrophoresis analysis of polymerase chain reaction-amplified genes coding for
737 16S rRNA. *Appl Environ Microbiol* 1993;**59**:695–700.

738 Neufeld JD, Vohra J, Dumont MG *et al.* DNA stable-isotope probing. *Nat Protoc* 2007;**2**:860–6.

739 Oksanen J, Blanchet FG, Friendly M *et al. Vegan: Community Ecology Package*., 2017.

740 Oyehan TA, Al-Thukair AA. Isolation and characterization of PAH-degrading bacteria from the Eastern
741 Province, Saudi Arabia. *Mar Pollut Bull* 2017;**115**:39–46.

742 Poonthrigpun S, Pattaragulwanit K, Paengthai S *et al.* Novel Intermediates of Acenaphthylene
743 Degradation by Rhizobium sp. Strain CU-A1: Evidence for Naphthalene-1,8-Dicarboxylic Acid
744 Metabolism. *Appl Env Microbiol* 2006;**72**:6034–9.

745 Sandrin TR, Maier RM. Impact of metals on the biodegradation of organic pollutants. *Environmental*
746 *Health Perspectives* 2003;**111**:1093-1101.

747 Sawulski P, Clipson N, Doyle E. Effects of polycyclic aromatic hydrocarbons on microbial community
748 structure and PAH ring hydroxylating dioxygenase gene abundance in soil. *Biodegradation*
749 2014;**25**:835–47.

750 Schloss PD, Westcott SL, Ryabin T *et al.* Introducing mothur: Open-Source, Platform-Independent,
751 Community-Supported Software for Describing and Comparing Microbial Communities. *Appl*
752 *Environ Microbiol* 2009;**75**:7537–41.

753 Smith VH, Graham DW, Cleland DD. Application of Resource-Ratio Theory to Hydrocarbon
754 Biodegradation. *Environ Sci Technol* 1998;**32**:3386–95.

755 Song M, Jiang L, Zhang D *et al.* Bacteria capable of degrading anthracene, phenanthrene, and
756 fluoranthene as revealed by DNA based stable-isotope probing in a forest soil. *J Hazard*
757 *Mater* 2016;**308**:50–7.

758 Storey S, Ashaari MM, Clipson N *et al.* Opportunistic Bacteria Dominate the Soil Microbiome
759 Response to Phenanthrene in a Microcosm-Based Study. *Front Microbiol* 2018;**9**, DOI:
760 10.3389/fmicb.2018.02815.

761 Sutherland JB. Detoxification of polycyclic aromatic hydrocarbons by fungi. *J Ind Microbiol*
762 1992;**9**:53–61.

763 Teng Y, Shen Y, Luo Y *et al.* Influence of Rhizobium meliloti on phytoremediation of polycyclic
764 aromatic hydrocarbons by alfalfa in an aged contaminated soil. *J Hazard Mater*
765 2011;**186**:1271–6.

766 Thion C, Cebron A, Beguiristain T *et al.* Long-term in situ dynamics of the fungal communities in a
767 multi-contaminated soil are mainly driven by plants. *Fems Microbiol Ecol* 2012a;**82**:169–81.

768 Thion C, Cébron A, Beguiristain T *et al.* PAH biotransformation and sorption by Fusarium solani and
769 Arthrobacter oxydans isolated from a polluted soil in axenic cultures and mixed co-cultures.
770 *Int Biodeterior Biodegrad* 2012b;**68**:28–35.

771 Thomas F, Corre E, Cébron A. Stable isotope probing and metagenomics highlight the effect of plants
772 on uncultured phenanthrene-degrading bacterial consortium in polluted soil. *ISME J* 2019,
773 DOI: 10.1038/s41396-019-0394-z.

774 Wald J, Hroudova M, Jansa J *et al.* Pseudomonads Rule Degradation of Polyaromatic Hydrocarbons in
775 Aerated Sediment. *Front Microbiol* 2015;**6**:1268.

776 Wang H, Lou J, Gu H *et al.* Efficient biodegradation of phenanthrene by a novel strain Massilia sp WF1
777 isolated from a PAH-contaminated soil. *Environ Sci Pollut Res* 2016;**23**:13378–88.

778 Wardle DA. A Comparative Assessment of Factors Which Influence Microbial Biomass Carbon and
779 Nitrogen Levels in Soil. *Biol Rev* 1992;**67**:321–58.

780 Wick LY, Ruiz de Munain A, Springael D *et al.* Responses of Mycobacterium sp. LB501T to the low
781 bioavailability of solid anthracene. *Appl Microbiol Biotechnol* 2002;**58**:378–85.

782 Zhang W, Chen L, Zhang R *et al.* High throughput sequencing analysis of the joint effects of BDE209-
783 Pb on soil bacterial community structure. *J Hazard Mater* 2016;**301**:1–7.

784 Zhang W, Wang H, Zhang R *et al.* Bacterial communities in PAH contaminated soils at an electronic-
785 waste processing center in China. *Ecotoxicology* 2010;**19**:96–104.

786 Zhou Z-F, Wang M-X, Zuo X-H *et al.* Comparative Investigation of Bacterial, Fungal, and Archaeal
787 Community Structures in Soils in a Typical Oilfield in Jianghan, China. *Arch Environ Contam*
788 *Toxicol* 2017;**72**:65–77.

789

790

Figure 1. Percentages of dissipated ^{13}C and degraded phenanthrene (PHE) at the end of SIP incubations (after 12 days*)*.
Error bars represent standard errors of the mean (n=3). Statistical differences (Kruskal-Wallis test, $p < 0.05$) of dissipated ^{13}C and degraded PHE among the soils are indicated by capital letters (different letters indicate significant differences). Significant difference (Welch's test) between degraded PHE and dissipated ^{13}C for one soil are indicated by stars, with *, ** and *** corresponding to $p < 0.05$, $p < 0.01$ and $p < 0.001$, respectively. Soils were ranked from left to right according to their total PAH concentration.

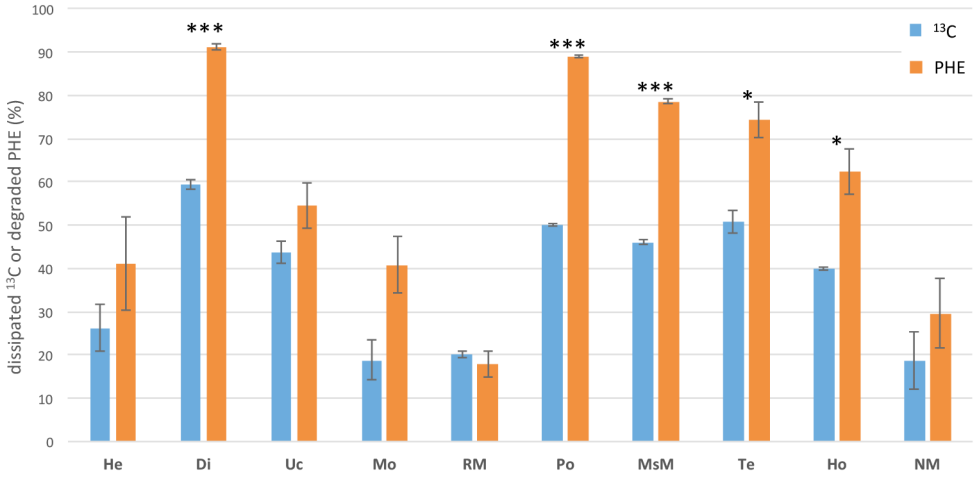

	He	Di	Uc	Mo	RM	Po	MsM	Te	Ho	NM	P-value
degraded PHE (%)	FG	A	EF	FG	H	AB	BC	CD	DE	GH	0.002
dissipated ^{13}C (%)	E	A	D	E	E	AB	CD	BC	D	E	0.002

Figure 2. Relations between the percentage of degraded PHE and biotic factors for unspiked soils or PHE-degrader characteristics found using SIP.
Correlation with total bacterial community Chao1 index (A) and bacterial abundance (B) of unspiked soils, PHE-degrader Shannon diversity index (C), and relative abundance of *Mycobacterium* taxa among PHE-degraders (D). No significant linear correlation was detected with PHE-degraders richness (E).

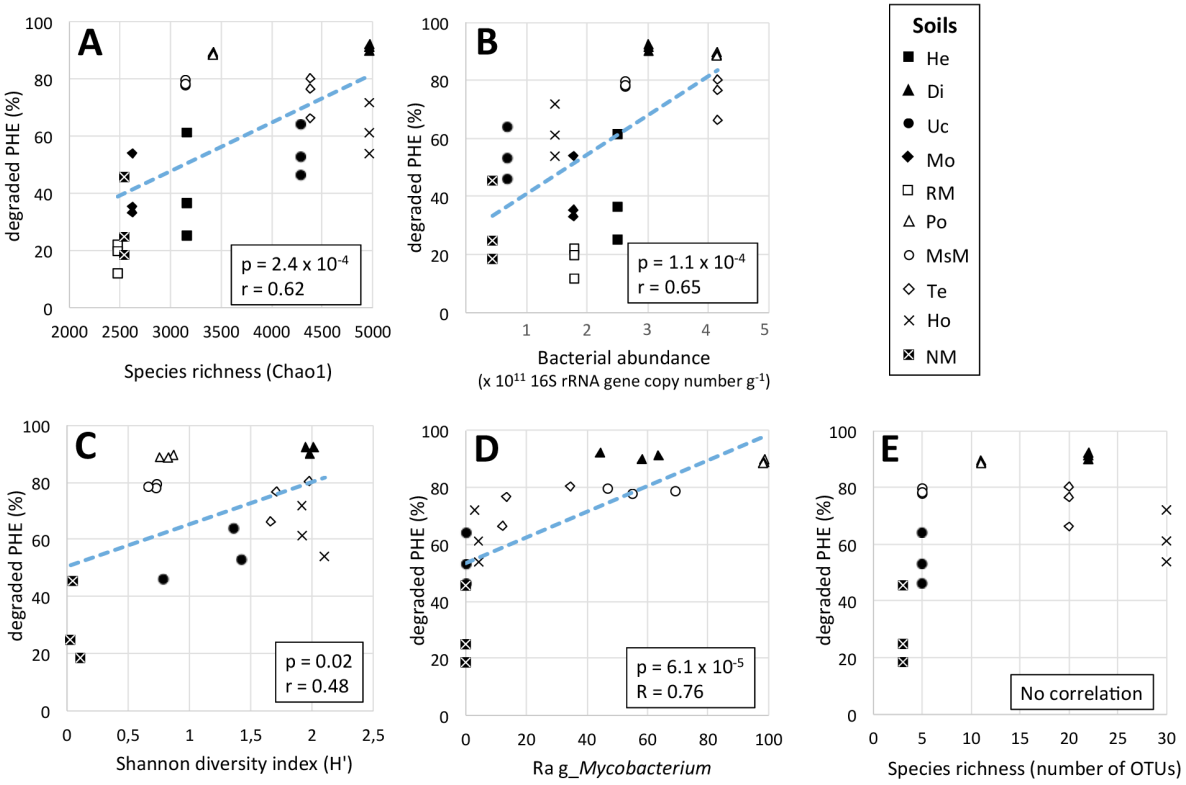

Figure 3. Quantification of bacterial 16S rRNA gene copy numbers in the 11 fractions (fractions n°1 and 13 were discarded) separated by CsCl gradients using real-time quantitative PCR in the ^{12}C (blue) and ^{13}C (orange) microcosms. Data are presented for the 10 soils of the collection. Error bars represent standard errors of the mean (n=3). Light and dark grey bars represent the light and heavy fractions used for PAH RDHAα gene quantification and enrichment calculations, respectively. Heavy DNAs corresponding to fractions 4 to 6 (highlighted by a dark grey bar) were selected for DNA sequencing.

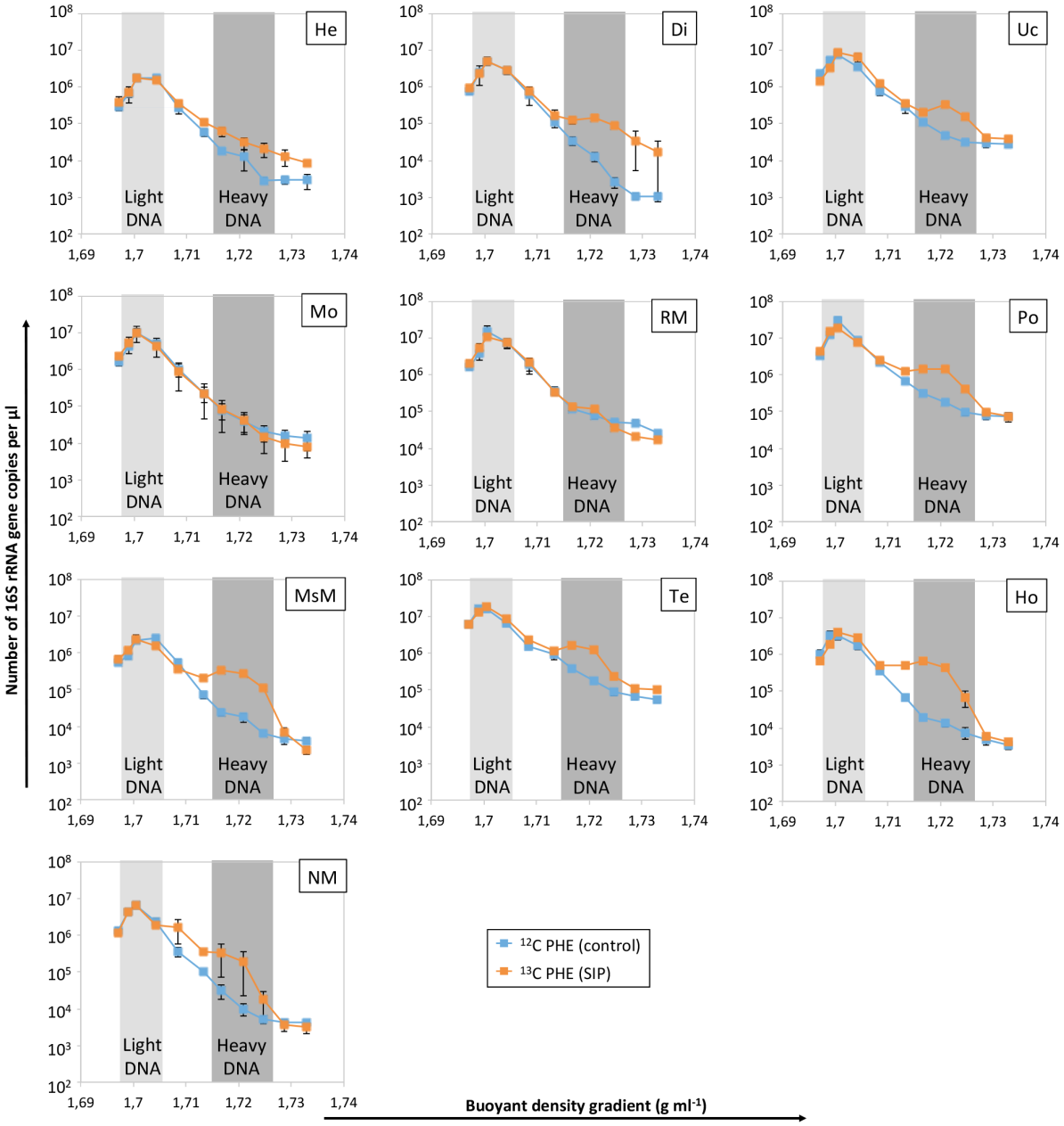

Figure 4. Active ^{13}C-labeled PHE degrading taxa identified in each soil, based on differential OTU abundance in heavy-DNA fractions between ^{13}C and ^{12}C-PHE incubations.
OTU having exactly the same taxonomic affiliation were summed as taxa groups. Their lowest possible classifications are given with the prefix corresponding to taxonomic rank (c =class, o = order, f = family, g = genus, no prefix = species). For each active PHE degrading taxa in one corresponding soil, Ra indicate the abundance relative to the whole pool of active PHE degraders identified through colour gradient, E indicates the enrichment factor of each taxa in ^{13}C-PHE compared to ^{12}C-PHE control through circle size (with the infinity symbol meaning that OTUs were only detected in ^{13}C- and not in ^{12}C-heavy DNA fractions), and N indicates the corresponding number of OTUs in the taxa groups. OTU groups originally classified as the Betaproteobacteriales order in the γ-Proteobacteria class (in Silva V132 database) are indicated here as β-Proteobacteria. Soils were ranked from left to right according to their total initial PAH concentration.

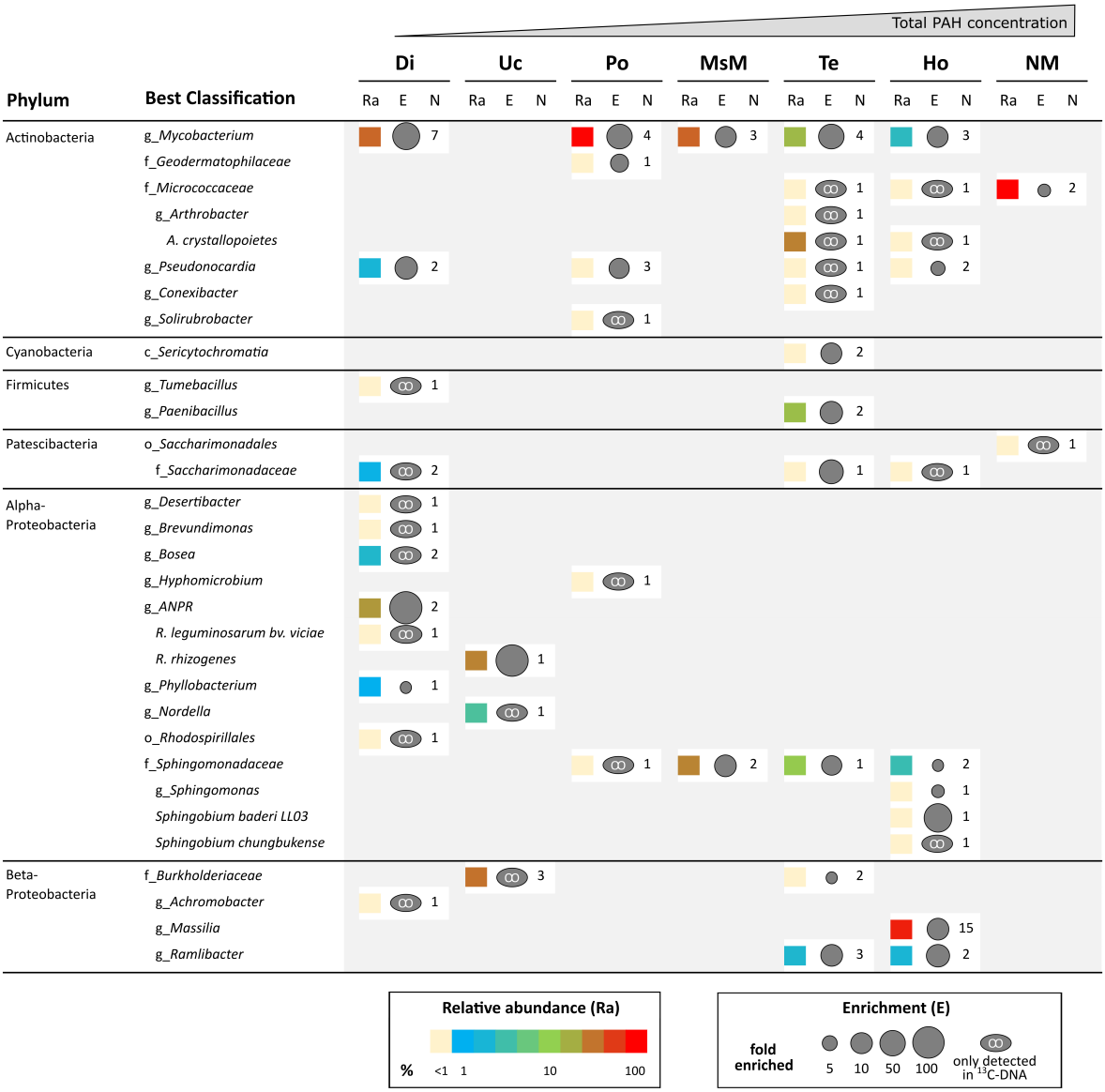

833

Table 1. PAH contents (sum of the 16 regulatory PAHs and of phenanthrene concentration) and PAH-degradation genes (PAH-RHDα GN and GP) copy numbers and abundances in the soils and in the sequenced ^{13}C-heavy DNA fraction, allowing to calculate functional gene enrichment in the ^{13}C-heavy DNA fraction consequently to the Stable Isotope Probing (SIP) incubations.

	Sum of 16 regulatory PAH (mg kg^{-1})		Phenanthrene (mg kg^{-1})		Percentage of functional gene copy relative to 16S rRNA genes						Gene enrichment during SIP incubation	
					In soils (before SIP incubation)		In soils (after SIP incubation)		In sequenced ^{13}C-heavy DNA fractions			
	Total	Available	Total	Available	PAH-RHDα GP (x 10^{-3})	PAH-RHDα GN (x 10^{-5})	PAH-RHDα GP (x 10^{-2})	PAH-RHDα GN (x 10^{-3})	PAH-RHDα GP	PAH-RHDα GN (x 10^{-3})	PAH-RHDα GP	PAH-RHDα GN
He	0.03 ± 0.01	<dl	<dl	<dl	7.0 ± 0.3	15.7 ± 1.0	5.7 ± 1.6	5.1 ± 2.6	0.3 ± 0.2	73.7 ± 10.5	8 ± 2	32 ± 16
Di	0.87 ± 0.06	<dl	0.11 ± 0.01	<dl	8.3 ± 0.4	11.5 ± 1.4	182.6 ± 23.0	N/A	39.4 ± 9.8	22.8 $^{+}$	221 ± 28	N/A
Uc	0.90 ± 0.09	<dl	0.26 ± 0.04	<dl	26.9 ± 3.6	14.0 ± 1.4	446.2 ± 27.6	1.0 ± 0.1	113.4 ± 28.9	18.3 ± 7.7	166 ± 10	7 ± 1
Mo	3.47 ± 1.35	<dl	1.34 ± 1.34	<dl	2.2 ± 0.2	4.9 ± 0.5	4.3 ± 0.6	0.5 ± 0.2	0.2 ± 0.1	18.7 $^{+}$	19 ± 3	11 ± 4
RM	6.59 ± 0.31	<dl	1.33 ± 0.03	N/A	11.2 ± 0.3	109.0 ± 9.3	26.6 ± 2.4	10.1 ± 1.4	1.9 ± 0.9	33.1 ± 16.7	24 ± 2	9 ± 1
Po	21.17 ± 2.33	0.18 ± 0.01	5.27 ± 2.79	<dl	22.1 ± 1.4	12.4 ± 0.8	462.7 ± 20.4	1.1 ± 0.4	81.1 ± 5.9	2.7 ± 0.8	209 ± 9	9 ± 3
MsM	49.65 ± 1.01	4.65 ± 0.62	4.40 ± 0.07	0.83 ± 0.06	31.4 ± 4.3	16.4 ± 4.7	505.1 ± 39.2	9.0 ± 0.8	24.5 ± 2.3	66.0 $^{+}$	161 ± 12	55 ± 5
Te	114.74 ± 0.50	6.31 ± 1.00	15.51 ± 0.09	0.88 ± 0.13	28.3 ± 3.0	6.1 ± 0.5	197.2 ± 22.4	7.7 ± 3.5	29.0 ± 6.4	2.2 ± 0.6	70 ± 8	126 ± 57
Ho	937.69 ± 14.31	54.14 ± 9.17	199.24 ± 3.25	18.10 ± 1.43	143.7 ± 12.2	329.0 ± 77.5	317.3 ± 29.3	159.2 ± 22.4	12.1 ± 3.1	274.9 ± 39.9	22 ± 2	48 ± 7
NM	1,095.90 ± 32.44	82.98 ± 8.47	104.08 ± 2.74	15.77 ± 0.56	160.5 ± 25.1	888.5 ± 475.6	69.9 ± 18.5	24.7 ± 8.0	0.9 ± 0.2	376.0 ± 197.6	4 ± 1	3 ± 1

Values are means (n = 3) ± standard errors of the mean (SEM). For values indicated by +, SEMs were not calculated because only one replicate showed results for gene quantification. <dl means lower than the detection limit.

845 **Figure S1.** Geographic localisation of the sites. *Blue, green, and red points correspond to weakly*
846 *anthropised, slag heap, and settling pond soils, respectively.*

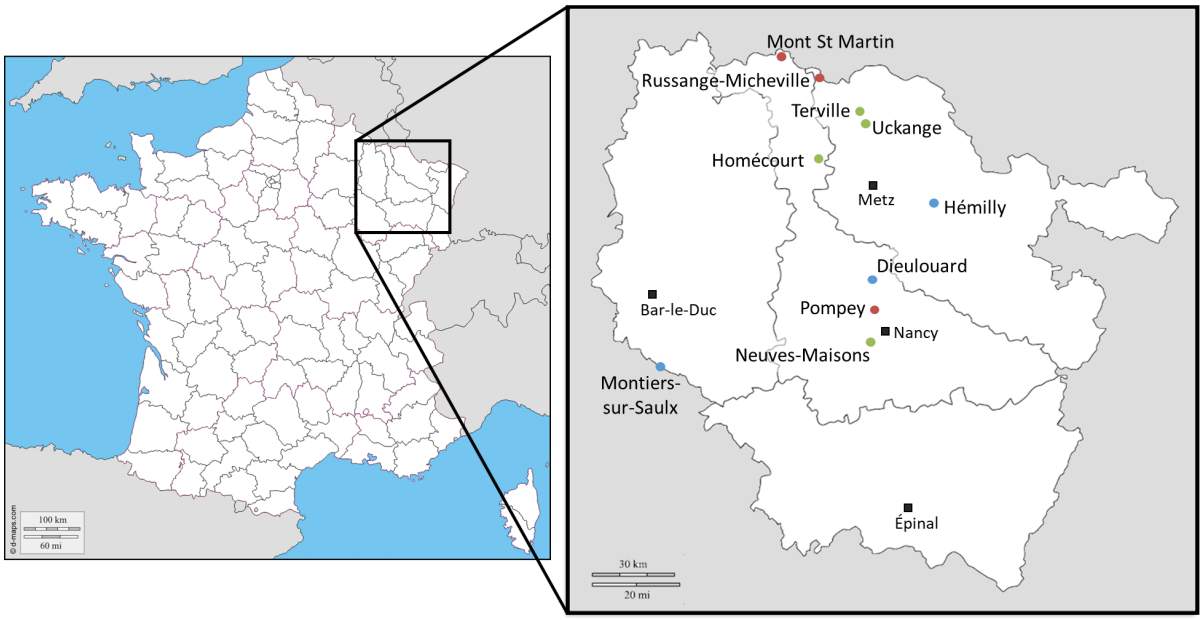

847

848

Figure S2. Soil respirations in the absence of a substrate (basal respiration, blue) or after phenanthrene spiking (orange), and differences in produced CO_2 (grey). *Basal respiration and respiration after PHE addition are expressed as cumulative curves and their values correspond to the left axis, whereas each difference in CO_2 production is represented at each time of measurement and their values correspond to the right axis. Error bars represent standard errors of the mean (n=3).*

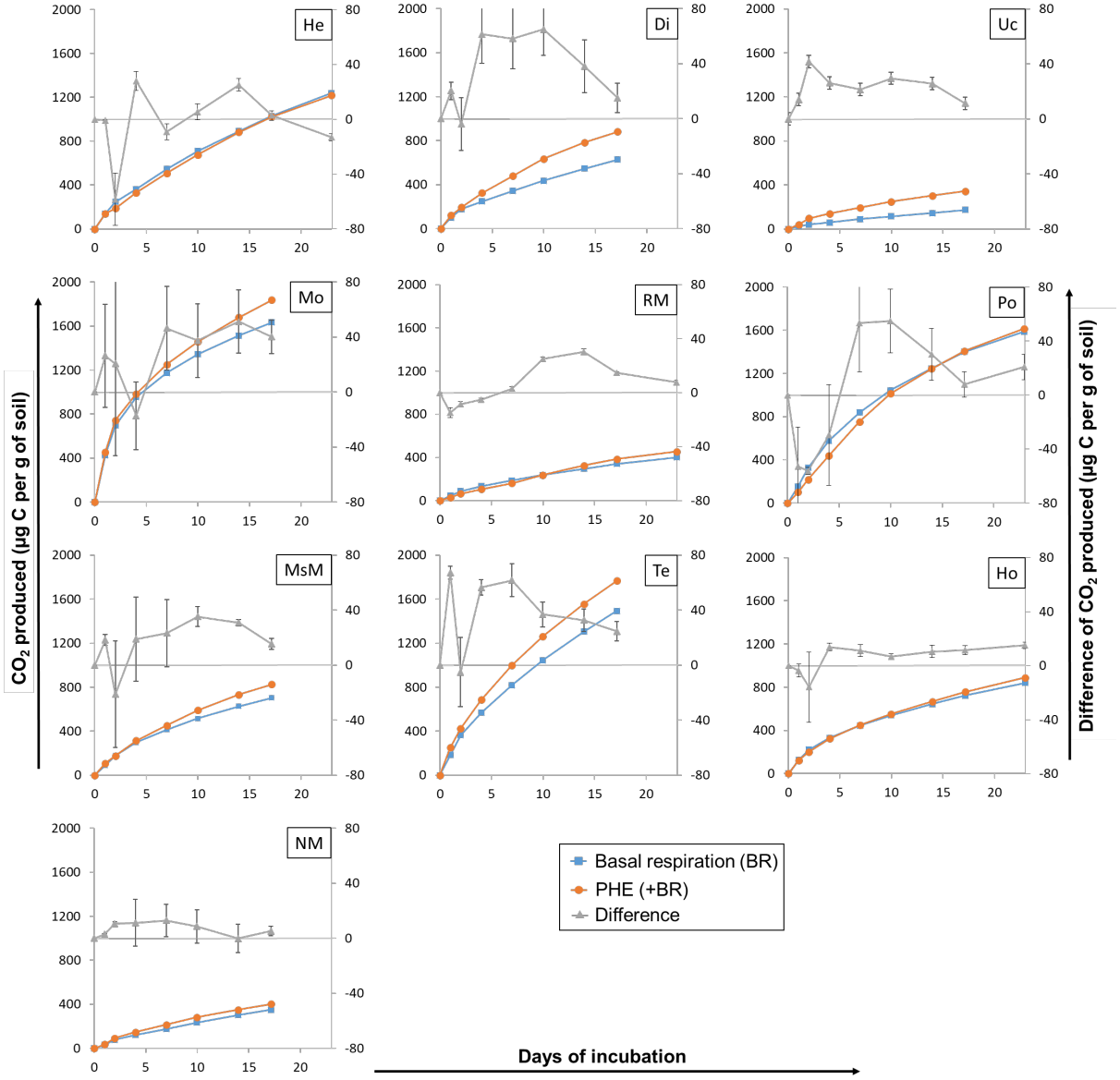

Table S1. Microbial and physico-chemical characteristics of unspiked soils. *16S rRNA gene copy numbers and Chao1 indices are represented by means (n = 3) ± standard errors of the mean (SEM). Zn, Pb, and Cd values correspond to total concentrations. From Lemmel et al. (2019).*

	16S rRNA Gene copy number per g dw soil (x 10^{10})	Chao1 richness index	pH (H_2O)	Total organic carbon (g kg^{-1})	Nitrogen (g kg^{-1})	C/N	Clay (%)	Silt (%)	Sand (%)	Zn (mg kg^{-1})	Pb (mg kg^{-1})	Cd (mg kg^{-1})
He	25.0 ± 2.2	3,162 ± 441	5.4	72.1	2.85	25.3	25.5	69.0	5.5	248	93	0.27
Di	30.1 ± 1.1	4,966 ± 56	7.3	24.3	1.74	14.0	11.5	14.3	74.2	60	31	0.15
Uc	6.8 ± 0.5	4,293 ± 505	8.0	29.9	0.56	53.6	5.5	17.6	76.9	74	23	0.09
Mo	17.8 ± 2.4	2,621 ± 356	7.0	81.5	4.56	17.9	48.9	46.0	5.1	144	44	0.71
RM	17.9 ± 0.4	2,478 ± 26	7.6	149.0	3.83	38.8	10.9	74.6	14.5	119,000	39,500	22.00
Po	41.5 ± 0.4	3,422 ± 386	7.8	109.0	7.19	15.2	17.5	53.3	29.2	29,600	34,700	152.00
MsM	26.4 ± 1.2	3,151 ± 4	7.2	119.0	4.18	28.5	10.9	72.7	16.4	55,400	14,400	17.60
Te	41.5 ± 1.2	4,381 ± 66	7.7	88.2	4.35	20.3	10.0	20.7	69.3	1,650	475	4.55
Ho	14.8 ± 0.7	4,966 ± 173	7.5	159.0	2.92	54.6	7.0	12.0	81.0	314	303	1.10
NM	4.4 ± 0.3	2,541 ± 174	7.4	75.2	2.35	32.0	13.3	27.9	58.8	2,540	653	3.27

Table S2. P-value and adjusted R-squared of the soil physicochemical characteristics tested in order to explain PHE degradation among soils. Based on simple linear correlations, the three soil characteristics showing the lowest P-values were selected to search for multiple interactions that could explain different PHE degradation rates among soils.

Explanatory variable	P-value	Adjust R-squared
P_Olsen	0.256	0.052
Cd_tot	0.265	0.046
C/N	0.281	0.036
P_Olsen * Cd_tot	0.185	0.292
P_Olsen * C/N	0.295	0.156
Cd_tot * C/N	0.396	0.054
P_Olsen * Cd_tot * C/N	0.568	0.041

Table S3. Richness, Shannon diversity and Pielou's evenness indices describing the active PHE-degrader's community diversity based on OTU identified through ^{13}C-DNA sequencing from Stable Isotope Probing incubations for the 7 soils studied.

	Richness index	Shannon diversity index	Pielou's evenness index
Di	22	1.98 ± 0.02	0.64 ± 0.01
Ho	30	1.98 ± 0.06	0.58 ± 0.02
MsM	5	0.71 ± 0.02	0.44 ± 0.01
NM	3	0.06 ± 0.02	0.06 ± 0.02

Po	11	0.82 ± 0.03	0.34 ± 0.01
Te	20	1.78 ± 0.10	0.59 ± 0.03
Uc	5	1.19 ± 0.20	0.74 ± 0.13

872

873